1984

Proton transfers between first- and second-row atoms: (H2OHSH2)+ and (H3NHSH2)+

Steve Scheiner
Utah State University

Proton transfers between first and second-row atoms: $(H_2OHSH_2)^+$ and $(H_3NHSH_2)^+$

Steve Scheiner[a)]
Department of Chemistry and Biochemistry, Southern Illinois University, Carbondale, Illinois 62901

(Received 23 March 1983; accepted 1 December 1983)

Ab initio molecular orbital methods are used to study the transfer of the central proton along the hydrogen bonds in $(H_2OHSH_2)^+$ and $(H_3NHSH_2)^+$. Proton transfer potentials are generated using the 4-31G* basis set at the Hartree–Fock level for various values for the hydrogen bond length R(XS). Full geometry optimizations are carried out at each stage of proton transfer. The barrier to proton transfer increases as the hydrogen bond is lengthened. For a given bond length, the highest barriers are observed for transfer from N to S and the smallest for the reverse process. Intermediate between these two extremes are transfers between O and S for which the forward and reverse transfers lead to nearly identical barrier heights. Adiabatic transfers, in which the intermolecular separation is allowed to change as the transfer progresses, are studied as well. The barrier to adiabatic transfer from OH_2 to SH_2 is 2.6 kcal/mol; 1.9 for the reverse process. Similar relaxation of R(NS) leads to no stable $(NH_3)(SH_3)^+$ structure and hence transfer from N to S is not expected. Application of larger basis sets and inclusion of correlation effects through second and third-order Møller–Plesset corrections support the reliability of the HF/4-31G* results.

During the past 15 years, a number of *ab initio* molecular orbital studies of proton transfer reactions[1–11] have greatly added to our understanding of this process. For example, electronic structures have been used[12–14] to rationalize observed comparative reaction rates and IR intensities and led to insights into enzymatic activity. However, the vast majority of these calculations have dealt with transfer of a proton between first-row atoms such as oxygen or nitrogen. It would be quite interesting to have at hand analogous information concerning second-row atoms in order to analyze the fundamental nature of the similarities and differences. It is ironic that since the first *ab initio* treatment of any proton transfer process, viz. Clementi's study[1] of H_3N–HCl, there has been little further investigation of transfers involving second-row atoms. With this in mind, the present communication reports calculations of proton transfer between first- and second-row atoms. Previous papers in this series[15–19] have analyzed transfers between simple hydrides of the first-row atoms such as OH_2 and NH_3. This paper extends the work to include transfers between these two molecules and SH_2, the analogous hydride of the second-row atom sulfur.

CHOICE OF METHOD

In studying the transfer energetics of a proton between two different molecules, it is imperative that the particular method used accurately reflect the relative proton affinities of these molecules. In a previous communication,[20] it was reported that the differences in experimental proton affinities between SH_2, OH_2, and NH_3 are very well reproduced by Hartree–Fock level calculations with the polarized split-valence basis set[20,21] 4-31G*. In fact, this agreement with experiment is comparable to that achieved by enlargement of the basis set to 6-311G** (including two sets of *d* functions) and incorporation of correlation effects by Møller–Plesset perturbation theory up to fourth order.[20] For this reason, most of the calculations reported herein were carried out at the HF/4-31G* level of theory.

In order to estimate the effects of basis set enlargement on the transfer process, calculations were also performed using a basis set of approximately triple-zeta plus polarization (TZP) quality. In addition, Møller–Plesset theory to second and third orders[22] was applied to gauge the magnitude of electron correlation effects. All calculations were performed using the GAUSSIAN-80 computer codes[23]; the gradient procedures contained therein were used for geometry optimizations.

RESULTS AND DISCUSSION

As a first step the geometries of the $(H_2OHSH_2)^+$ and $(H_3NHSH_2)^+$ complexes were fully optimized at the HF/4-31G* level. The parameters used to describe the geometries of these C_s structures are illustrated in Fig. 1. The separation between the O or N first-row atom (X) and S is denoted as R in both cases; y is the distance of the central proton H^c above the X–S internuclear axis. α_O and α_S specify the angles between the X–S axis and the OH_2 and SH_2 bisectors, respectively.

The fully optimized geometries of the two complexes are provided in the first rows of Tables I and II along with the SCF energy of each. The equilibrium R(XS) distances in the fully optimized structures are 3.022 Å for $(H_2OHSH_2)^+$

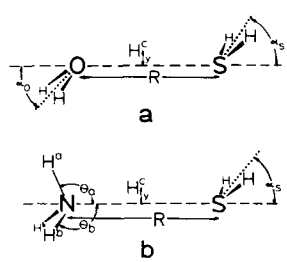

FIG. 1. Geometries of $(H_2OHSH_2)^+$ and $(H_3NHSH_2)^+$. Both structures belong to the C_s point group. Dotted lines represent bisectors of OH_2 and SH_2 moieties.

[a)] Recipient of NIH Research Career Development Award (1982–1987).

 0021-9606/84/051982-06$02.10

TABLE I. Optimized geometries[a] and energies for $(H_2OHSH_2)^+$ and monomers.

R	r(OH[c])	r(OH)	r(SH)	θ(HOH)	θ(HSH)	α_O	α_S	y	
			$(H_3OHSH_2)^+$						E^{SCF}(a.u.)
3.022	1.037	0.964	1.345	111.1	94.2	44.3	77.7	0.007	−474.508 92
			$(H_3O)^+ + SH_2$						E^D(kcal/mol)
		0.972	1.343	113.0	93.3				23.2 (19.4)[b]
									24.9[c]
			$H_2O + (SH_3)^+$						E^D(kcal/mol)
		0.948	1.353	105.3	95.7				21.8 (16.7)[b]
									21.9[c]

[a] All bond lengths in Å, angles in degrees.
[b] Corrected for zero-point energies, etc. (see the text).
[c] Experimental values from Ref. 24.

and 3.350 Å for $(H_3NHSH_2)^+$. In both cases, the equilibrium position of the central proton is much closer to the first-row atom than to sulfur with respective r(XH[c]) bond lengths of 1.037 and 1.033 Å. These minimum energy structures may therefore be denoted as $(OH_3)^+(SH_2)$ and $(NH_4)^+(SH_2)$.

Also included in Tables I and II are the optimized geometries of the monomers from which the two complexes may be considered as arising by hydrogen-bond formation. Dissociation of the complexes to neutral SH_2 and the protonated cation $(OH_3)^+$ or $(NH_4)^+$ is described in the first set while the last row involves dissociation to $(SH_3)^+$ and the neutral first-row hydride. The energies required for the indicated dissociations are listed as E^D in the last column of the tables. For the $(H_2OHSH_2)^+$ system, dissociation to $OH_2 + (SH_3)^+$ is favored over $(OH_3)^+ + SH_2$ by some 1.4 kcal/mol due to the slightly greater proton affinity of SH_2. Also included (in parentheses) are dissociation energies corrected for zero-point vibrational energies, losses of translational and rotational degrees of freedom, and $\Delta(PV)$. The resulting H-bond energies for $(H_2OHSH_2)^+$ are somewhat smaller than the experimental values,[24] perhaps due to neglect of electron correlation.

Proton transfer potentials for the $(H_2OHSH_2)^+$ and $(H_3NHSH_2)^+$ systems are presented in Figs. 2 and 3, respectively. These curves were generated in the following manner. An R(XS) separation was chosen and held fixed as the central proton was moved towards the S atom. For each step in the transfer, i.e., for each value of r(XH[c]), the remainder of the molecular geometry was fully optimized.

For the equilibrium value of R(OS) = 3.02 Å, the transfer potential in Fig. 2 is of double-well type and is very nearly symmetrical. The left well corresponding to $(OH_3)^+(SH_2)$ is slightly lower in energy than that for $(OH_2)(SH_3)^+$, somewhat surprising in light of the greater proton affinity of SH_2 than of OH_2. It is interesting that the situation reverses and the right-hand well is a bit more stable for greater R(OS) separations. Besides the slight alteration in asymmetry, the lengthening of R(OS) leads to substantial increases in the height of the energy barrier separating the two wells. Also worthy of note is the fact that the potential collapses into a single-well function when R(OS) is contracted to 2.8 Å.

The much higher proton affinity of NH_3 produces the high degree of asymmetry in the proton transfer potential curves of $(H_3NHSH_2)^+$ in Fig. 3. The right-hand well is rather shallow for the equilibrium R(NS) separation of 3.35 Å. As this distance is increased, the right minimum becomes more clearly defined as the barrier separating it from the left-hand well increases.

The calculated barriers to proton transfer $E^\dagger$ are listed in Table III for the two systems. The shorthand notation OH→S refers to the transfer of a proton from OH_2 to SH_2 in $(H_2OHSH_2)^+$ while SH→O corresponds to reverse motion from the right-hand minima of Fig. 2 to the left. Similar notation is used for $(H_3NHSH_2)^+$. The rise in barrier height associated with increased R(XS) separation is clearly illustrated in Fig. 4. For equivalent values of R, the highest barriers are observed for NH→S and the lowest for the reverse process. Intermediate between these two extremes are transfers between O and S for which the near symmetry of the potential curves leads to approximately equal barriers. The

TABLE II. Optimized geometries[a] and energies for $(H_3NHSH_2)^+$ and monomers.

R	r(NH[c])	r(NH[a])	r(NH[b])	r(SH)	θ_a	θ_b	θ(HSH)	α_S	y	
				$(H_3NHSH_2)^+$						E^{SCF}(a.u.)
3.350	1.033	1.012	1.012	1.344	113.5	107.8	94.1	70.7	0.063	−454.752 59
			r(NH)	r(SH)	θ(HNH)	θ(HSH)				
				$(NH_4)^+ + SH_2$						E^D(kcal/mol)
			1.014	1.343	109.47	93.3				13.9(12.7)[b]
				$NH_3 + (SH_3)^+$						E^D(kcal/mol)
			1.003	1.353	107.0	95.7				55.1(48.8)[b]

[a] All bond lengths in Å, angles in degrees.
[b] Corrected (see the text).

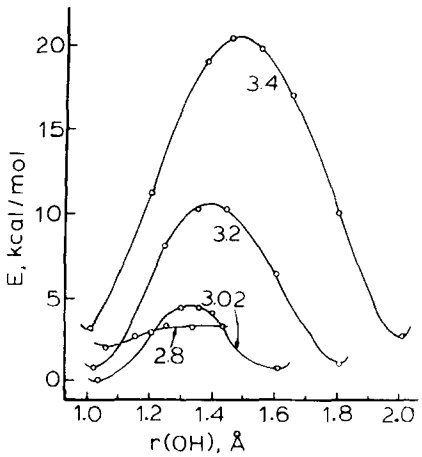

FIG. 2. Potential energy curves for proton transfer in $(H_2OHSH_2)^+$. The numerical label on each curve corresponds to the R(OS) distance (in Å). All energies are shown relative to the fully optimized structure with R(OS) = 3.02 Å.

intercept of the SH→O curve with the horizontal axis at about R = 2.9 Å corresponds to the absence of a barrier in the single-well potential for $(H_2OHSH_2)^+$ at this intermolecular separation. The right-hand minimum vanishes for $(H_3NHSH_2)^+$ for R(NS) distances of about 3.3 Å, only slightly shorter than the equilibrium separation of 3.35 Å.

Geometry changes during transfer

Previous studies[15,18] of proton transfers involving OH_2 and NH_3 have led to the conclusion that geometry optimizations at each stage of transfer are not essential for accurate elucidation of the energetics. More specifically, transfer potentials calculated using the "rigid molecule" approximation, wherein all nuclei with the exception of the central proton are frozen in their equilibrium positions, were only slightly different than those calculated including geometry optimizations throughout. The magnitudes of the changes in geometry undergone by the $(H_2OHSH_2)^+$ system during the proton transfer are explored in Table IV. The R(OS) distance was held fixed at 3.2 Å and the central proton moved in

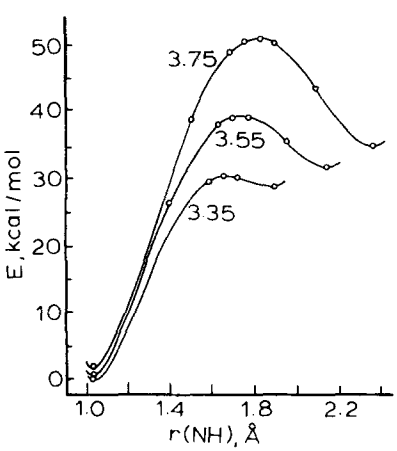

FIG. 3. Proton transfer potentials for $(H_3NHSH_2)^+$. Labels refer to R(NS) in Å. Energies relative to fully optimized structure.

TABLE III. Energy barriers to proton transfer.

R (Å)	$E^\dagger$ (kcal/mol)		R (Å)	$E^\dagger$ (kcal/mol)	
	OH→S	SH→O		NH→S	SH→N
3.02[a]	4.6	3.8	3.35[a]	30.4	1.7
3.20	9.8	9.5	3.55	39.1	7.8
3.40	17.4	17.7	3.75	49.0	16.0

[a] Equilibrium intermolecular distance.

stages toward the S atom, as indicated by the values of $r(OH^c)$ in the first column. The remainder of the parameters were all optimized.

During the course of the transfer, the OH bond length of the water unit undergoes a smooth decrease of some 0.013 Å while r(SH) lengthens by 0.005 Å. The HOH bond angle contracts by 5° and a smaller increase of 1° is noted in θ(HSH). Perhaps the most radical change is undergone by α_O which describes the angle between the HOH bisector and the O–S axis. This angle decreases by 37° while a much smaller increase of 5° occurs in α_S. It should also be noted that the path of the central proton does not lie precisely along the line between the O and S atoms but within about 0.02 Å of this axis. When close to the O, H^c lies above the axis but quickly shifts below it until it reaches the S.

The geometry changes occurring during the proton transfer in $(H_3NHSH_2)^+$ are provided in Table V for the R(NS) distance of 3.55 Å. These changes are rather similar to those described above for $(H_2OHSH_2)^+$ although generally of smaller magnitude. The NH bond lengths in the proton donor molecule are reduced by 0.007 Å as compared to twice that amount in OH_2. The increases in the θ_a and θ_b angles correspond to a decrease in the internal θ(HNH) bond angle of 3° compared to a 5° reduction in θ(HOH). Changes in the internal geometry of SH_2 are much the same as in the prior case of $(H_2OHSH_2)^+$. The angle between the SH_2 plane and the N–S axis α_S goes through a greater increase (10°) than the 5° rise noted for $(H_2OHSH_2)^+$. The path followed by the transferring proton lies always above the N–S axis, generally by about 0.01 Å.

Geometry optimizations were found to be quite essential for accurate calculation of the energetics of proton transfer in $(H_2OHSH_2)^+$. As an example, for R(OS) = 3.022 Å (the equilibrium distance) the calculated barrier including geometry optimizations is 4.57 kcal/mol. If, instead of following this procedure, the transfer is carried out using the rigid molecule approximation wherein the entire structure of

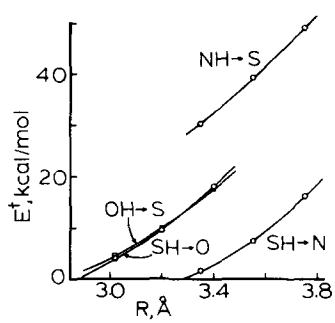

FIG. 4. Energy barriers to proton transfer as a function of R(XS). Arrows indicate direction of proton transfer in associated hydrides. For example, NH→S refers to transfer from NH_3 to SH_2.

TABLE IV. Optimized geometrical parameters during proton transfer in $(H_2OHSH_2)^+$ for R(OS) = 3.2 Å.[a]

r(OH^c)	r(OH)	r(SH)	θ(HOH)	θ(HSH)	α_O	α_S	y
1.019	0.965	1.345	111.4	94.1	48.0	76.5	0.021
1.25	0.961	1.346	109.8	94.3	46.1	80.2	−0.006
1.35	0.959	1.347	109.1	94.4	43.9	81.3	−0.011
1.45	0.956	1.348	108.5	94.6	39.7	81.2	−0.015
1.60	0.954	1.349	107.6	94.8	29.9	82.0	−0.014
1.808	0.952	1.350	106.3	95.2	11.0	81.9	−0.020

[a] All distances in Å, angles in degrees.

the complex is fixed in its equilibrium geometry, the barrier is increased to 4.94 kcal/mol. Much more striking, however, is the discrepancy between barriers for the reverse SH→O transfer. The rigid molecule approximation leads to a barrier 40% lower than the value of 3.80 kcal/mol obtained with geometry optimizations throughout. The situation is rather different for $(H_3NHSH_2)^+$ where the rigid molecule approximation leads to only small errors in calculated energetics. For the three R(NS) distances examined and for transfers in either the NH→S or SH→N directions, the differences between full optimization and rigid molecule barriers are around 1 kcal/mol or less.

Adiabatic transfers

The proton transfer potentials reported above were obtained for given values of R(XS) which were fixed during the course of the transfer. This treatment is appropriate when the transfer takes place via very rapid proton tunneling or when the hydrogen bond is contained within a macromolecular structure which does not allow optimum approach of the two groups involved in the bond. It is also of interest, however, to consider an "adiabatic" transfer process in which the proton moves slowly enough that all other nuclei can adjust their positions at each stage of transfer. Calculations were therefore carried out to study this adiabatic transfer by performing full geometry optimizations of $(H_2OHSH_2)^+$, *including* R(OS), for a series of values of r(OH^c). These results are presented in Table VI where it may be seen that the adiabatic transfer of a proton from OH_2 to SH_2 involves an initial contraction of R(OS) which reaches a minimum value of 2.87 Å at the midpoint of the transfer. It is at this point that the relative energy attains a maximum of 2.6 kcal/mol which is the barrier to adiabatic transfer. Concurrent with a continuation of the proton transfer process and the associated decrease in energy is a reenlargement of R(OS) to 3.062 Å in the equilibrium geometry of $(OH_2)(SH_3)^+$. The barrier for the reverse process, i.e., adiabatic transfer from S to O, is somewhat smaller at 1.9 kcal/mol. A similar treatment of $(H_3NHSH_2)^+$ leads to a monotonically increasing energy as the proton is transferred from NH_3 to SH_2 and the conclusion that this system does not contain a stable $(H_3N–HSH_2)^+$ structure.

Basis set and correlation effects

It would be useful to estimate the effects on the results reported here of using larger basis sets and including electron correlation. The basis set was accordingly enlarged up to the triple-zeta 6-311G* level[25] which includes a set of *d* functions ($\zeta = 1.292$) on oxygen. Dunning's [6*s*4*p*] contraction[26] of Huzinaga's (11*s*7*p*) set[27] of primitive Gaussians was used for S and was augmented by a single set of *d* functions ($\zeta = 0.6$). This basis set is abbreviated as TZP in the following. Electron correlation was explicitly evaluated using Møller–Plesset perturbation theory to second (MP2) and third (MP3) orders.[22] Rather than attempting to perform extremely time-consuming geometry optimizations at levels of theory higher than HF/4-31G*, the calculations were performed directly upon the geometries optimized at that level.

The specific subject of the calculations was the $(H_2OHSH_2)^+$ system at the fixed R(OS) distance of 3.2 Å, shown above to contain barriers of 9.8 and 9.5 kcal/mol for OH→S and SH→O transfer, respectively. Calculations were performed upon both the optimized $(H_2OH–SH_2)^+$ and $(H_2O–HSH_2)^+$ geometries in the first and final rows of Table IV and on the midpoint of the transfer as well. The energy barriers are reported in Table VII for each level of calculation.

TABLE V. Changes in optimized geometry[a] during proton transfer in $(H_3NHSH_2)^+$, R(NS) = 3.55 Å.

r(NH^c)	r(NH^a)	r(NH^b)	r(SH)	θ_a	θ_b	θ(HSH)	α_S	y
1.03	1.012	1.012	1.343	112.6	108.0	94.0	70.5	0.051
1.40	1.008	1.008	1.345	109.7	108.7	94.2	78.0	0.009
1.63	1.006	1.006	1.346	110.6	109.2	94.5	80.7	0.010
1.70	1.005	1.005	1.347	111.1	109.5	94.6	81.0	0.010
1.77	1.005	1.005	1.348	111.7	109.9	94.7	81.3	0.010
1.95	1.005	1.005	1.349	113.0	110.8	95.0	81.3	0.010
2.14	1.005	1.005	1.350	114.2	111.3	95.3	80.9	0.007

[a] All distances in Å, angles in degrees.

TABLE VI. Full geometry optimizations[a] of $(H_2OHSH_2)^+$ for a series of values of $r(OH^c)$. Energies are shown relative to the equilibrium structure.

$r(OH^c)$	R(OS)	r(OH)	r(SH)	θ(HOH)	θ(HSH)	α_O	α_S	y	E(kcal/mol)
1.037	3.022	0.964	1.345	111.1	94.2	44.3	77.7	+0.007	0
1.20	2.900	0.960	1.347	109.6	94.4	40.0	80.1	−0.017	2.2
1.25	2.880	0.959	1.347	109.2	94.6	36.9	80.6	−0.022	2.6
1.30	2.874	0.958	1.348	108.8	94.6	33.5	81.1	−0.026	2.6
1.35	2.880	0.956	1.348	108.4	94.7	29.9	81.1	−0.026	2.4
1.40	2.894	0.955	1.348	108.2	94.8	24.3	81.0	−0.023	2.1
1.50	2.945	0.954	1.349	107.5	95.0	19.6	81.2	−0.021	1.3
1.660	3.062	0.953	1.350	106.8	95.1	12.0	81.3	−0.019	0.7

[a] All distances in Å, angles in degrees.

It is first clear from the data that at any level of theory, enlargement of basis set leads to an increase in barrier height. Electron correlation has an opposite effect and produces a sizable reduction. The barrier lowering observed with MP3 is somewhat smaller than second-order reductions. These qualitative conclusions are in nice agreement with results obtained[16–19] with other systems like $(HOHOH)^-$ and $(H_3NHNH_3)^+$. Because of the large numbers of basis orbitals and electrons involved, MP3 calculations were not performed for the larger TZP basis set. The values in parentheses in Table VII were arrived at by the following reasoning. It has been demonstrated previously[28] that the effects of basis set extension and of electron correlation are largely separable and additive. For example, as indicated in the first row of Table VII, enlargement of the basis set from 4-31G* to TZP increases the OH→S transfer barrier at the Hartree–Fock level by 3.2 kcal/mol from 9.8 to 13.0. A similar increase is observed at the MP2 level. (Conversely, inclusion of second-order MP corrections lowers the barrier by about 4.8 kcal/mol with either the 4-31 G* or TZP basis sets.) It is thus reasonable to conclude that similar parallelism will apply to the MP3 level and that the MP3/4-31G* barrier of 6.2 kcal/mol will be increased to about 9.3 with the larger basis set. It is anticipated that further enlargement of basis set will lead to additional small increases in the barrier height such that the HF/4-31G* value of 9.8 provides an extremely accurate estimate.

The additivity of basis set and correlation effects appears to be valid also for the reverse SH→O transfer although not quite as precisely as in the previous case. The barrier increases resulting from basis set enlargement at the HF and MP2 levels differ by 0.8 kcal/mol. If we estimate the enlargement occurring at the MP3 level to be 2.8 kcal/mol, we arrive at a value of 7.4 for MP3/TZP. After the further increases expected for additional enlargement of basis set, we may expect the HF/4-31G* value to be a slight overestimate of the SH→O barrier height.

TABLE VII. Calculated energy barriers (kcal/mol) for proton transfer in $(H_2OHSH_2)^+$ with R(OS) = 3.2 Å.

	OH→S			SH→O		
	4-31G*	TZP	Δ	4-31G*	TZP	Δ
HF	9.8	13.0	3.2	9.5	11.7	2.2
MP2	5.0	8.1	3.1	3.4	6.4	3.0
MP3	6.2	(9.3)[a]		4.6	(7.4)[a]	

[a] Estimated (see the text).

CONCLUSIONS

At the equilibrium intermolecular separations 3.02 Å for $(H_2OHSH_2)^+$ and 3.35 Å for $(H_3NHSH_2)^+$ double-well potentials are associated with proton transfers in both systems. Consistent with previous findings for other systems,[15–19] the energy barriers to proton transfer rise with increasing hydrogen bond length. The high basicity of NH_3 leads to very asymmetric potential curves in $(H_3NHSH_2)^+$ and to much higher barriers for transfer from NH_3 to SH_2 than for the reverse direction. The approximately equal proton affinities of OH_2 and SH_2 are reflected in nearly symmetric transfer potentials and very similar barriers for transfer in either direction in $(H_2OHSH_2)^+$.

Geometry optimizations during the course of proton transfer point out significant alterations within each monomer such as reductions in the OH bond length and HOH bond angle in water as the proton is transferred to SH_2. More dramatic are changes in the intermolecular orientation, particularly α_O, the angle between the HOH plane and the O–S internuclear axis. These geometry changes lead to the failure of the rigid molecule approximation to provide energy barriers in good agreement with those calculated including geometry optimizations during the transfer in $(H_2OHSH_2)^+$. Although the geometry changes occurring in $(H_3NHSH_2)^+$ are by no means insignificant, energy barriers to proton transfer calculated using the rigid molecule approximation provide excellent estimates of those including relaxation of the geometries.

Without the restriction of fixed intermolecular distance, the potential energy surface of $(H_3NHSH_2)^+$ does not contain a stable $(NH_3)(SH_3)^+$ structure. On the other hand, both $(OH_3)^+(SH_2)$ and $(OH_2)(SH_3)^+$ correspond to minima in the surface of $(H_2OHSH_2)^+$. The adiabatic barrier to "slow" proton transfer from the first minimum to the second is 2.6 kcal/mol. The reverse process is exothermic by 0.7 kcal/mol, with a barrier of 1.9. As observed previously in other systems, enlargement of basis set leads to increase in the barrier to proton transfer while a reduction arises from inclusion of electron correlation. The net result is that the HF/4-31G* barriers provide excellent estimates of the values calculated using much more costly theoretical approaches.

ACKNOWLEDGMENTS

Financial support was provided by the National Institute of General Medical Sciences (GM29391) and the Research Corporation. Allocations of computer time from the SIU Computing Center are acknowledged.

[1]E. Clementi, J. Chem. Phys. **46**, 3851 (1967).
[2]J. J. Delpuech, G. Serratrice, A. Strich, and A. Veillard, Mol. Phys. **29**, 849 (1975).
[3]P. Merlet, S. D. Peyerimhoff, and R. J. Buenker, J. Am. Chem. Soc. **94**, 8301 (1972).
[4]G. H. F. Diercksen, W. von Niessen, and W. P. Kraemer, Theor. Chim. Acta **31**, 205 (1973).
[5]K. Pecul, Theor. Chim. Acta **44**, 77 (1977); K. Pecul and R. Janoschek, *ibid.* **36**, 25 (1974).
[6]P. A. Kollman and L. C. Allen, J. Am. Chem. Soc. **92**, 6101 (1970).
[7]M. D. Newton and S. Ehrenson, J. Am. Chem. Soc. **93**, 4971 (1971).
[8]B. O. Roos, W. P. Kraemer, and G. H. F. Diercksen, Theor. Chim. Acta **42**, 77 (1976).
[9]W. Meyer, W. Jakubetz, and P. Schuster, Chem. Phys. Lett. **21**, 97 (1973).
[10]A. Støgård, A. Strich, J. Almlöf, and B. Roos, Chem. Phys. **8**, 405 (1975).
[11]G. Karlström, B. Jönsson, B. Roos, and H. Wennerström, J. Am. Chem. Soc. **98**, 6851 (1976).
[12]M. N. Paddon-Row, C. Santiago, and K. N. Houk, J. Am. Chem. Soc. **102**, 6561 (1980); A. Laforgue, C. Brucena-Grimbert, D. Laforgue-Kantzer, G. Del Re, and V. Barone, J. Phys. Chem. **86**, 4436 (1982); S. Nagaoka, N. Hirota, T. Matsushita, and K. Nishimoto, Chem. Phys. Lett. **92**, 498 (1982); F. Keil and R. Ahlrichs, J. Am. Chem. Soc. **98**, 4787 (1976).
[13]R. Janoschek, E. G. Weidemann, and G. Zundel, J. Chem. Soc. London Faraday Trans. 2 **69**, 505 (1973); R. Janoschek, Theor. Chim. Acta **29**, 57 (1973); R. Janoschek, E. G. Weidemann, H. Pfeiffer, and G. Zundel, J. Am. Chem. Soc. **94**, 2387 (1972); H. Pfeiffer, G. Zundel, and E. G. Weidemann, J. Phys. Chem. **83**, 2544 (1979).
[14]A. Warshel and R. M. Weiss, J. Am. Chem. Soc. **102**, 6218 (1980); P. A. Kollman and D. M. Hayes, *ibid.* **103**, 2955 (1981); S. Scheiner and W. N. Lipscomb, Proc. Natl. Acad. Sci. U.S.A. **73**, 432 (1976).
[15]S. Scheiner, J. Chem. Phys. **77**, 4039 (1982); J. Phys. Chem. **86**, 367 (1982).
[16]M. M. Szcześniak and S. Scheiner, J. Chem. Phys. **77**, 4586 (1982).
[17]S. Scheiner, M. M. Szcześniak, and L. D. Bigham, Int. J. Quantum Chem. **23**, 739 (1983).
[18]S. Scheiner, J. Am. Chem. Soc. **103**, 315 (1981); Ann. N.Y. Acad. Sci. **367**, 493 (1981).
[19]S. Scheiner and L. B. Harding, J. Am. Chem. Soc. **103**, 2169 (1981); J. Phys. Chem. **87**, 1145 (1983).
[20]S. Scheiner, Chem. Phys. Lett. **93**, 540 (1982).
[21]R. Ditchfield, W. J. Hehre, and J. A. Pople, J. Chem. Phys. **54**, 724 (1971); W. J. Hehre, R. Ditchfield, and J. A. Pople, *ibid.* **56**, 2257 (1972); J. B. Collins, P. von R. Schleyer, J. S. Binkley, and J. A. Pople, *ibid.* **64**, 5142 (1976).
[22]J. S. Binkley and J. A. Pople, Int. J. Quantum Chem. **9**, 229 (1975); J. A. Pople, J. S. Binkley, and R. Seeger, *ibid.* **10**, 1 (1976).
[23]J. S. Binkley, R. A. Whiteside, R. Krishnan, R. Seeger, D. J. DeFrees, H. B. Schlegel, S. Topiol, L. R. Kahn, and J. A. Pople, QCPE, GAUSSIAN-80, Program No. 406 (1981).
[24]K. Hiraoka and P. Kebarle, Can. J. Chem. **55**, 24 (1977).
[25]B. Krishnan, J. S. Binkley, J. S. Seeger, and J. A. Pople, J. Chem. Phys. **72**, 650 (1980).
[26]T. H. Dunning, Jr. and P. J. Hay, in *Methods of Electronic Structure Theory*, edited by H. F. Schaefer (Plenum, New York, 1977), pp. 1–27.
[27]S. Huzinaga, Department of Chemistry Report, University of Alberta, Edmonton, Alberta, Canada, 1971.
[28]R. H. Nobes, W. J. Bouma, and L. Radom, Chem. Phys. Lett. **89**, 497 (1982); R. H. Nobes, W. R. Rodwell, W. J. Bouma, and L. Radom, J. Am. Chem. Soc. **103**, 1913 (1981); M. L. McKee and W. N. Lipscomb, *ibid.* **103**, 4673 (1981); J. A. Pople, R. Krishnan, H. B. Schlegel, and J. S. Binkley, Int. J. Quantum Chem. **14**, 545 (1978).